

## Supporting Information

### Highly Hydrophobic Metal–Organic Framework for Self-Protecting Gate Dielectrics

Arif I. Inamdar,<sup>a,b,c</sup> Abhishek Pathak,<sup>a</sup> Muhammad Usman,<sup>a</sup> Kuan-Ru Chiou,<sup>d</sup> Pei-Hsien Tsai,<sup>a</sup> Shruti Mendiratta,<sup>a</sup> Saqib Kamal,<sup>a</sup> Yen-Hsiang Liu,<sup>e</sup> Jenq-Wei Chen,<sup>d</sup> Ming-Hsi Chiang,<sup>a</sup> and Kuang-Lieh Lu<sup>\*a,e</sup>

<sup>a</sup>Institute of Chemistry, Academia Sinica, Taipei 115, Taiwan

<sup>b</sup>Department of Applied Chemistry, National Chiao Tung University, Hsinchu 300, Taiwan

<sup>c</sup>Sustainable Chemical Science and Technology, Taiwan International Graduate Program, Academia Sinica and National Chiao Tung University, Taipei 115, Taiwan

<sup>d</sup>Department of Physics, National Taiwan University, Taipei 106, Taiwan

<sup>e</sup>Department of Chemistry, Fu Jen Catholic University, New Taipei City 242, Taiwan

#### Table of Contents

1) SEM images .....	(S2)
2) Crystal structure, PXRD and BET surface area.....	(S3-S5)
3) Dielectric and electrical conductivity graphs .....	(S6-S8)
4) Crystal data and structural refinement .....	(S9)

## 1.0 SEM images

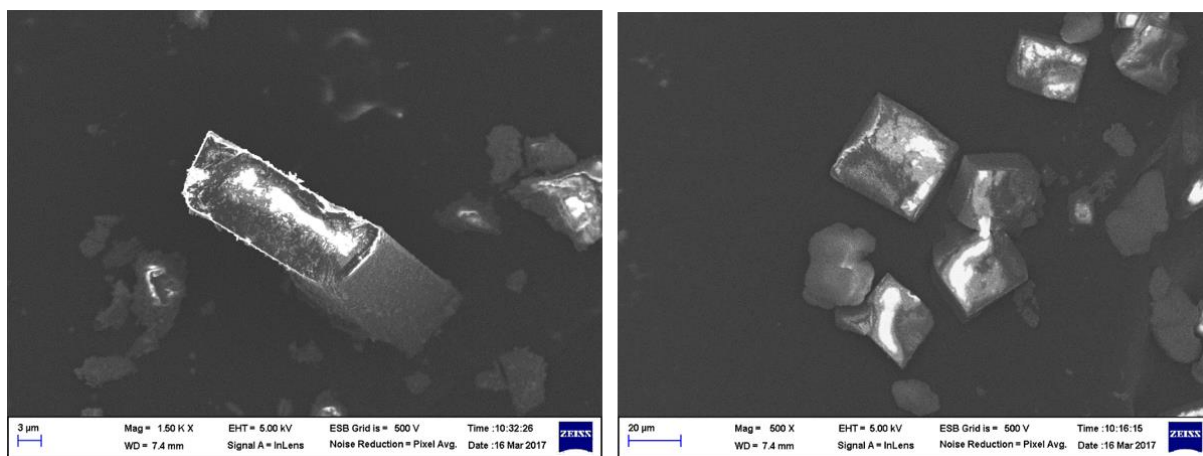


**Fig. S1** Scanning electron microscope images of compound **1**.

## 2.0 Crystal structure, PXRD and contact angle images

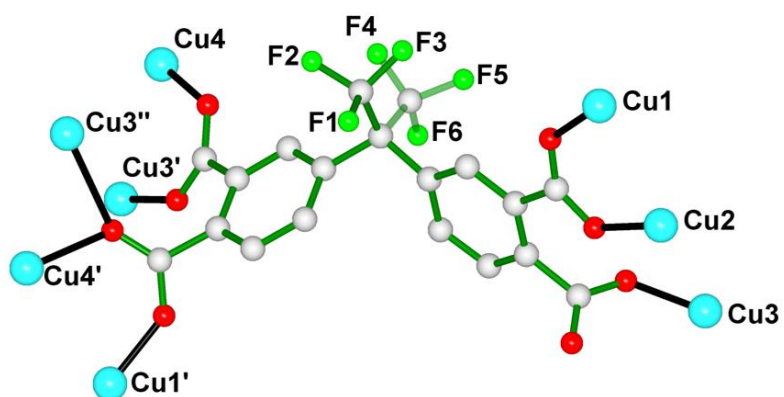


Fig. S2 Coordination of four different copper atoms.

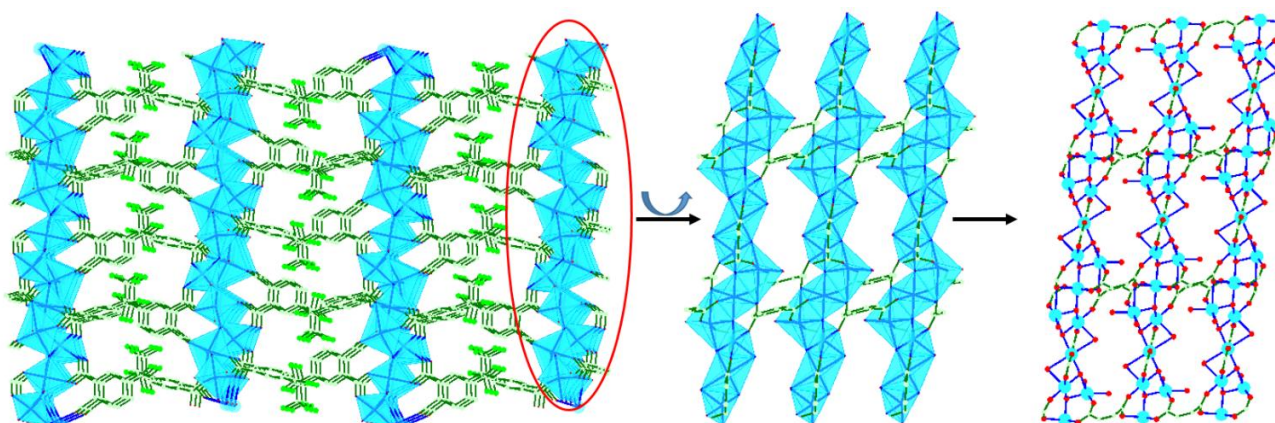


Fig. S3 Two dimensional layer of the metal oxide chain.

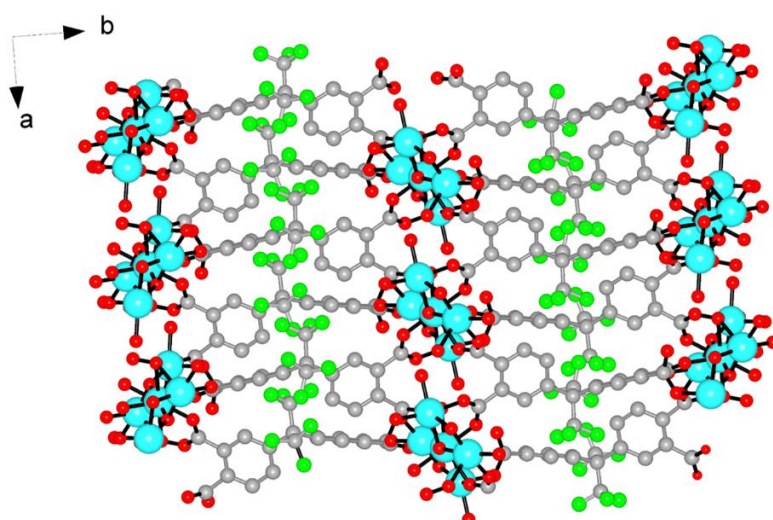
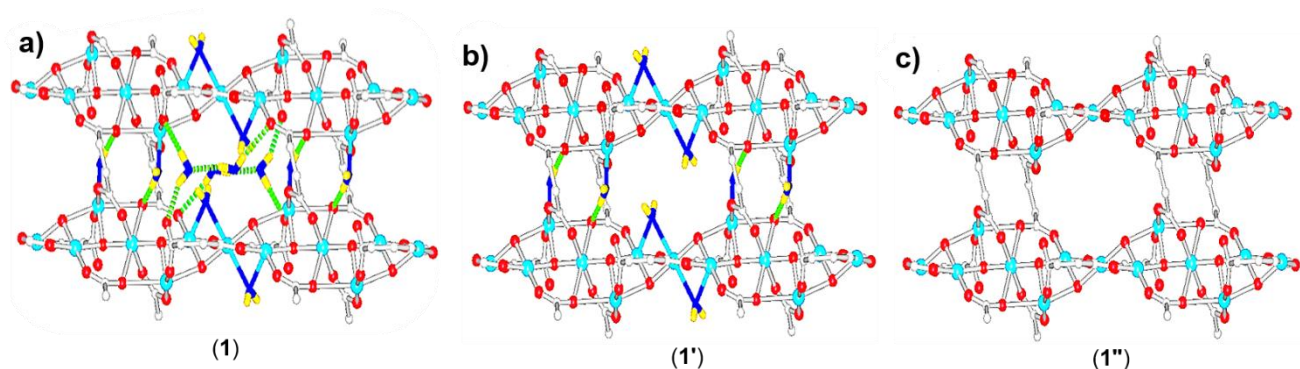


Fig. S4 Structure of compound 1 along the c-axis.



**Fig. S5** a) Hydrogen bonding interactions between guest water, oxide chain and coordinated water. b) Structure of compound **1'** based on compound **1** which showing hydrogen bonding interactions of coordinated water molecules with oxide chain. c) Structure of compound **1''** based on compound **1**, oxide chain free from hydrogen bonding interactions of guest and coordinated water molecules.

### 3.0 Powder X-ray and thermogravimetric analysis

The powder X-ray diffraction data for the three compounds in (Fig. 2b) in precisely matched the simulated X-ray data for compound **1**. Activation of compound **1** done at two different temperatures 140 °C and 170 °C resulted in the formation of compound **1'** and compound **1''**, respectively. In the case of 170 °C, compound **1''** was in a completely dehydrated state, as evidenced by TGA data and PXRD data showed that an older peak had disappeared and a newer one was formed, indicating that this was final stage of dehydration for compound **1**. Compound **1'**, an intermediate state of compound **1**, underwent a phase transition and a new peak was formed (Fig. S6). Thermogravimetric analyses of compound **1**, compound **1'** and compound **1''** in the temperature range 30–800 °C were performed (Fig. 2a). The TGA data for compound **1** showed a one step weight loss of 9.50% between 155–267 °C. The percentage weight loss coincides with the calculated value of guest and coordinated water molecules.

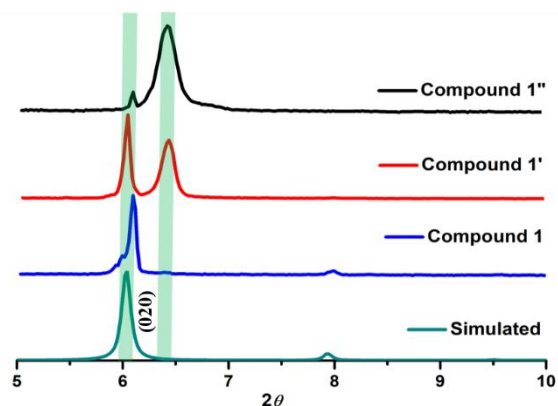


**Fig. S6** Enlarged picture of the PXRD for compounds **1**, **1'**, and **1''**.

#### 4.0 BET surface area and FT-IR

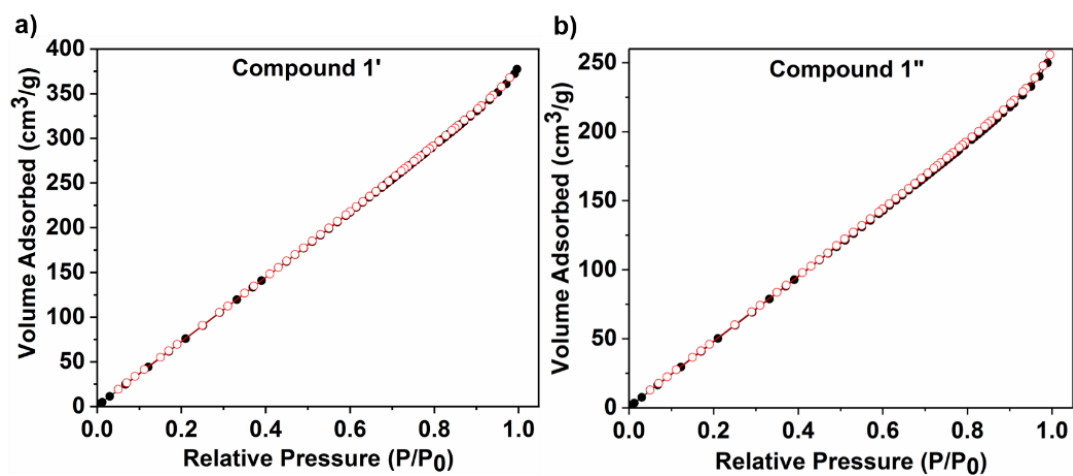


Fig. S7 Nitrogen gas adsorption isotherm of 1' and 1''.

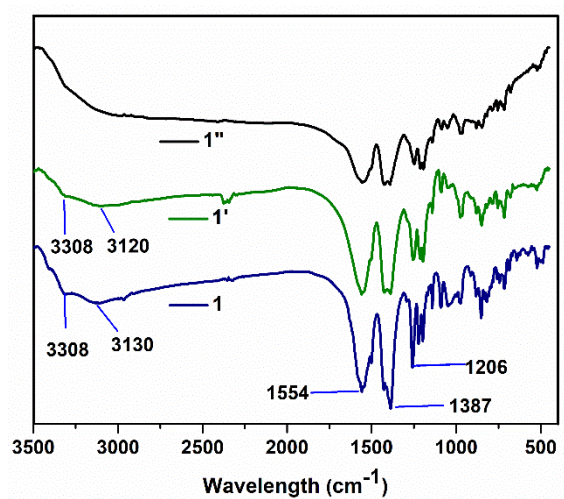
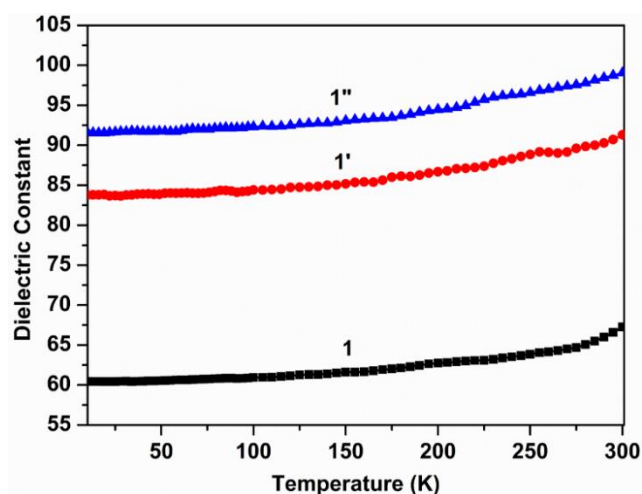


Fig. S8 FT-IR spectra of compounds 1, 1' and 1''.

## 5.0 Dielectric and electrical conductivity graphs

### 5.1 Dielectric constant



**Fig. S9** Temperature dependent dielectric constants of compounds **1**, **1'** and **1''** at 1 kHz.

### 5.2 Dielectric relaxation

The dielectric relaxation of compounds **1**, **1'**, and **1''** at 300 K and 1 kHz are 67.44, 91.29, and 98.99, respectively, and for 1 MHz are 57.54, 79.18 and 86.20.

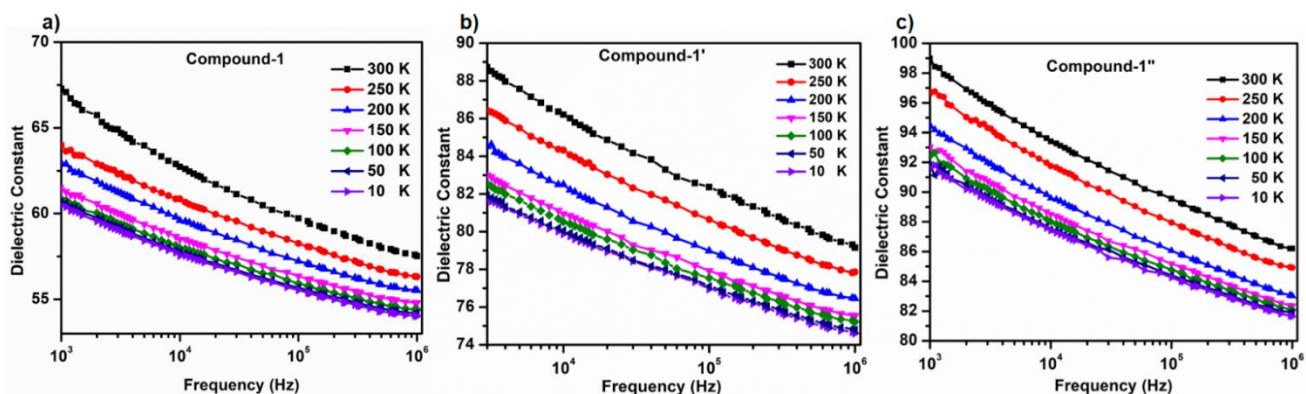


**Fig. S10** Frequency dependent dielectric constants of compound **1** (a), **1'** (b) and **1''** (c) at different temperatures.

### 5.3 Dielectric loss versus temperature

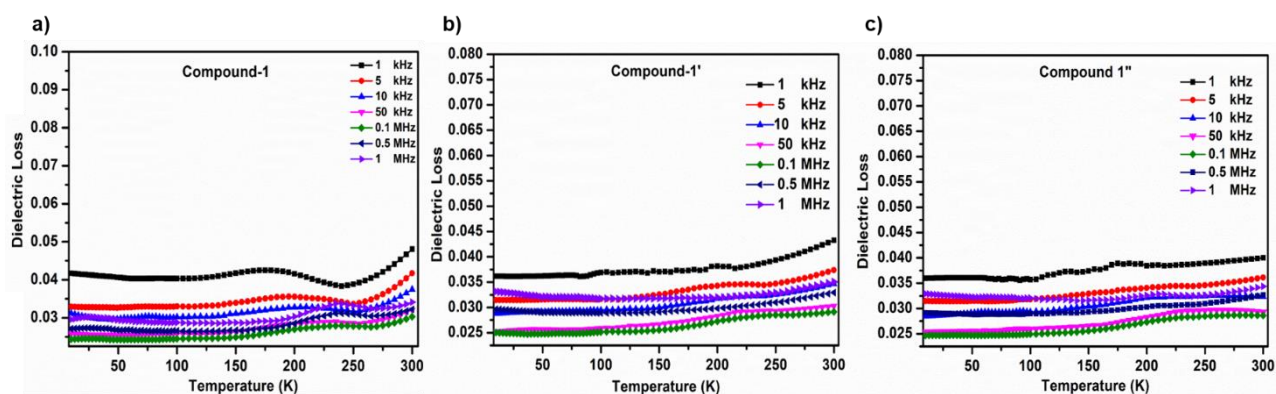


**Fig. S11** Temperature dependent dielectric loss of compound **1** (a), **1'** (b), and **1''** (c) at different frequencies.

### 5.4 Dielectric loss versus frequency

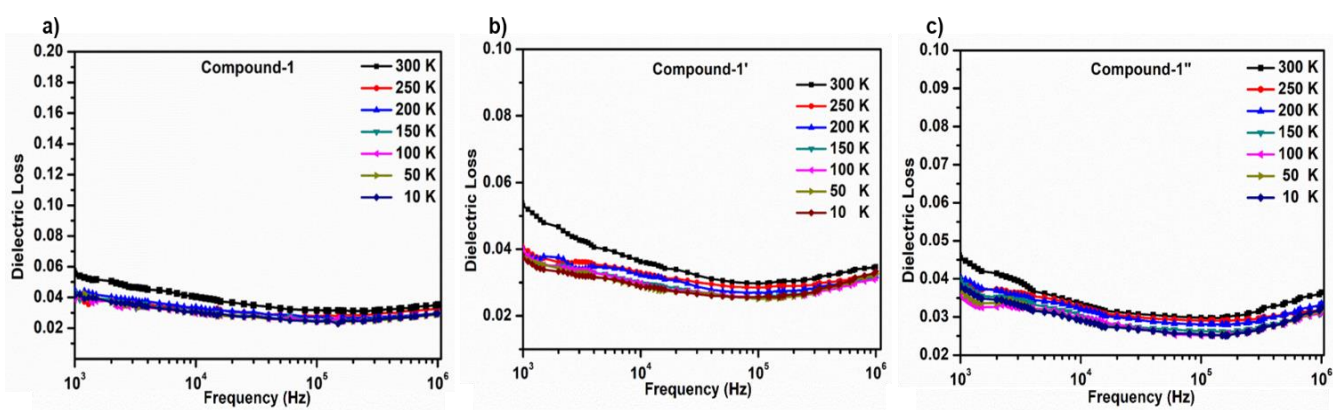


**Fig. S12** Frequency dependent dielectric loss of compound **1** (a), **1'** (b), and **1''** (c) at different temperatures.

## 5.5 Electrical conductivity versus temperature

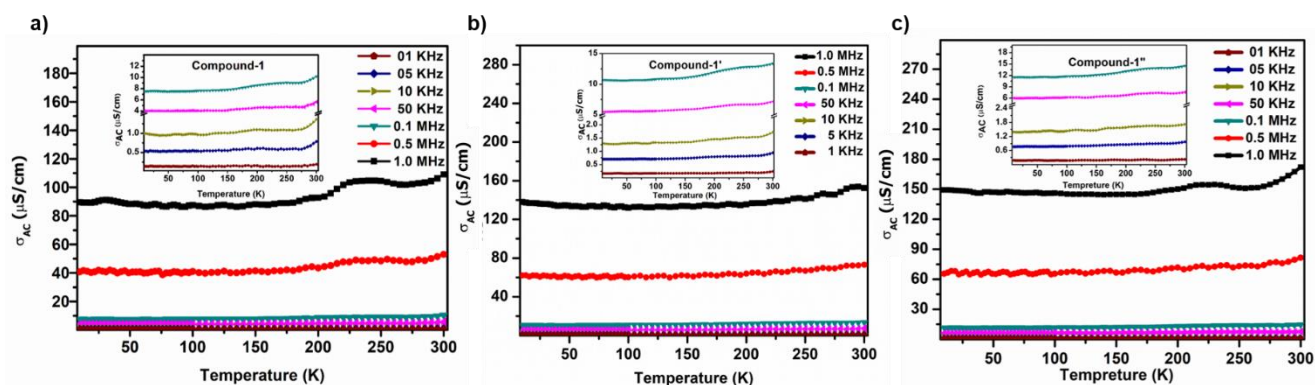


**Fig.S13** Temperature dependent electrical conductivities of compound **1** (a), **1'** (b), and **1''** (c) at different frequencies.

## 5.6 Electrical conductivity versus frequency

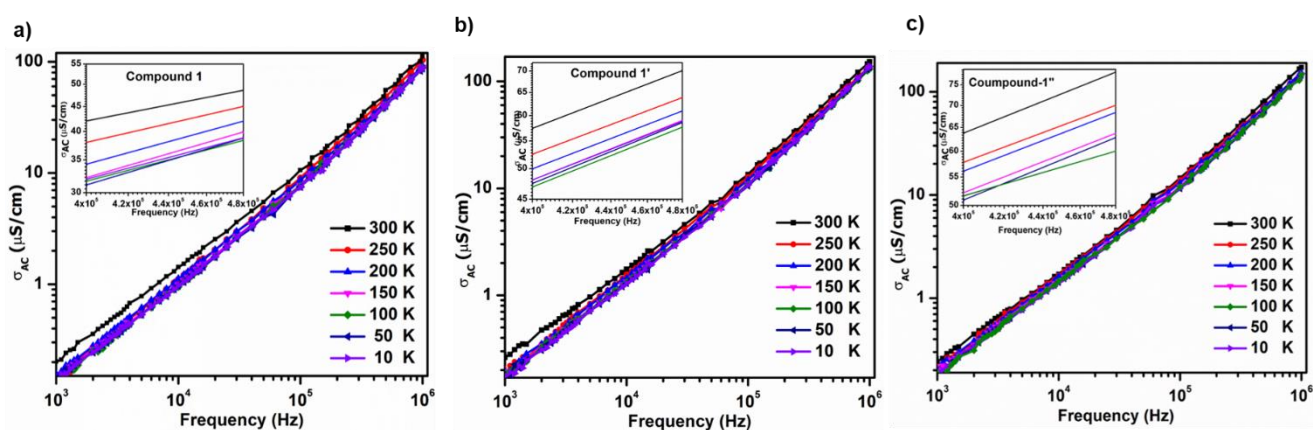


**Fig. S14** Frequency dependent electrical conductivities of compound **1** (a), **1'** (b), and **1''** (c) at different temperatures.

## 6.0 Crystal Data of Compound 1 (CCDC 1840045)

**Table S1.** Crystal and structure refinement data for compound 1

Empirical formula	C38 H28 Cu6 F12 O28
Formula weight	1541.84
Temperature	200(2) K
Wavelength	0.71073 Å
Crystal system	Monoclinic
Space group	$P2_1/n$
Unit cell dimensions	$a = 7.1011(2)$ Å $b = 29.2707(9)$ Å $c = 12.1221(3)$ Å $\beta = 96.8380(10)^\circ$
Volume	$2501.71(12)$ Å <sup>3</sup>
Z	2
Density (calculated)	$2.047$ Mg/m <sup>3</sup>
Absorption coefficient	$2.643$ mm <sup>-1</sup>
$F(000)$	1524
Crystal size	$0.14 \times 0.12 \times 0.02$ mm <sup>3</sup>
Theta range for data collection	$2.19$ to $25.06^\circ$
Index ranges	$-8 \leq h \leq 8$ , $-34 \leq k \leq 34$ , $-14 \leq l \leq 14$
Reflections collected	50821
Independent reflections	4436 [R(int) = 0.0465]
Completeness to theta = $25.06^\circ$	99.6%
Absorption correction	multi-scan
Max. and min. transmission	0.9490 and 0.7085
$R_1$ , $wR_2$ [ $I > 2\sigma(I)$ ] <sup>a</sup>	$R_1 = 0.0307$ , $wR_2 = 0.0699$
$R_1$ , $wR_2$ (all data) <sup>a</sup>	$R_1 = 0.0433$ , $wR_2 = 0.0790$

$$^a R_1 = \frac{\sum ||F_0| - |F_c||}{\sum |F_0|}; wR_2 = \frac{[\sum w(F_0^2 - F_c^2)_2]}{[\sum w(F_0^2)_2]}^{1/2}$$

## 7.0 Crystal Data of HFDPA Ligand (CCDC 1955564)

**Table S2.** Crystal and structure refinement data for hydrolysed HFDPA ligand

Empirical formula	C <sub>19</sub> H <sub>16</sub> F <sub>6</sub> O <sub>11</sub>
Formula weight	534.32
Temperature	200(2) K
Wavelength	0.71073 Å
Crystal system	Monoclinic
Space group	<i>C2/c</i>
Unit cell dimensions	$a = 39.860(4)$ Å $b = 17.4023(18)$ Å $c = 13.4692(14)$ Å $\beta = 100.218(3)^\circ$
Volume	9194.8(17) Å <sup>3</sup>
<i>Z</i>	16
Density (calculated)	1.544 Mg/m <sup>3</sup>
Absorption coefficient	0.156 mm <sup>-1</sup>
<i>F</i> (000)	4352
Crystal size	0.20 x 0.18 x 0.02 mm <sup>3</sup>
Theta range for data collection	2.30 to 25.04°
Index ranges	-47 ≤ <i>h</i> ≤ 46, 20 ≤ <i>k</i> ≤ 19, -16 ≤ <i>l</i> ≤ 16
Reflections collected	60896
Independent reflections	8095 [R(int) = 0.1158]
Completeness to theta = 25.06°	99.5%
Absorption correction	multi-scan
Max. and min. transmission	0.9969 and 0.9695
R <sub>1</sub> , wR <sub>2</sub> [ <i>I</i> > 2σ( <i>I</i> )] <sup>a</sup>	R <sub>1</sub> = 0.0650, wR <sub>2</sub> = 0.1557
R <sub>1</sub> , wR <sub>2</sub> (all data) <sup>a</sup>	R <sub>1</sub> = 0.1297, wR <sub>2</sub> = 0.1809

$$^a R_1 = \frac{\sum ||F_0| - |F_c||}{\sum |F_0|}; wR_2 = \left[ \frac{\sum w(F_0^2 - F_c^2)_2}{\sum w(F_0^2)_2} \right]^{1/2}$$

## References

- S1. L. J. Farrugia. *J. Appl. Cryst.* 1999, **32**, 837–838.
- S2. G. M. Sheldrick. *Acta Cryst.* 2015, **C71**, 3–8.
- S3. G. M. Sheldrick. *Acta Cryst.* 2008, **A64**, 112–122.
- S4. A. L. Spek. *Acta Cryst.* 2015, **C71**, 9–18.